Encyclopaedia of Quaternary Science, 3rd Edition

Methane Studies in Ice Cores

Rachael Rhodes, Department of Earth Sciences, University of Cambridge, Downing Site, Cambridge, CB2 3EQ, UK.
rhr34@cam.ac.uk

Abstract

This article presents state-of-the-art atmospheric methane reconstruction based on ice core studies. Starting with a biogeochemical overview of the methane cycle, it presents and discusses the anthropogenic impact on atmospheric CH_4. It then introduces the processes of gas diffusion in firn and trapping in ice and their impact on methane reconstructions. The trends of this greenhouse gas and its isotopic composition over the last two thousand years, the Holocene, the Last Glacial and deglaciation, and the last eight glacial–interglacial cycles are summarised, and likely drivers are discussed. Analytical techniques and non-atmospheric signal artifacts are also briefly described.

Keywords
Antarctica, Anthropogenic impact, Atmospheric composition, Biogeochemical cycles, Biomass burning, Climate dynamics, Dansgaard-Oeschger events, Glacial-interglacial cycles, Greenland, Holocene, Ice cores, Methane

Key Points

1. Ice cores record atmospheric methane mixing ratio and isotopic composition over timescales from decades to glacial-interglacial cycles.
2. Human activity has caused methane to more than double since 1750 CE to levels not seen in the last 800,000 years.
3. The natural methane budget past and present is dominated by sources in the tropical regions, predominantly wetlands.
4. In the Last Glacial, rapid methane increases occurred in tandem with repeated abrupt Arctic warming events.
5. Methane varies with global climate over orbital timescales between 320 parts per billion (ppb) in glacial periods to 800 ppb in interglacials.

Introduction

Current understanding of the methane cycle

Methane (CH_4) is a trace gas in our atmosphere with a globally averaged mixing ratio of >1912 ppb. It is also a powerful greenhouse gas, molecule-per-molecule more potent than carbon dioxide (CO_2), but with a relatively short atmospheric lifetime of around a decade, which reduces its radiative forcing impact over longer timescales. Human activity has increased methane levels by >150% since 1750 CE, equivalent to 0.54 W m^{-2} of radiative forcing (Arias et al., 2021).

Earth's methane budget is a balance of its emissions from sources and removal by sinks. The dominant sink is oxidation with the short-lived hydroxyl radical (OH) in the troposphere, which accounts for ~90% of CH_4 removal. Remaining methane removal occurs via chemical reactions in the stratosphere, reactions with chlorine in the troposphere, and in soils via the action of methanotrophic bacteria. It is notoriously difficult to quantify variations in sink strength over time, even in the recent past where air can be directly sampled. The consensus between atmospheric chemistry modelling and atmospheric measurements linked to OH abundance seems to be that OH levels did not change between 1850 and 1980 CE but increased up to 2014 CE (Stevenson et al., 2020). Beyond the era of direct atmospheric measurements, CH_4 sink strength is unknown; several modelling studies argue it has stayed relatively constant across key climate transitions (Levine et al., 2012, 2011; Murray et al., 2014) and in general ice core CH_4 studies adopt this view.

Decomposition of organic matter in anoxic environments of the terrestrial biosphere is the source of the majority of CH_4 emissions to the atmosphere under pre-industrial conditions. Wetland regions ranging from tropical mangroves to boreal peat bogs are the major CH_4 emitters (~150 Tg CH_4 yr^{-1}) (Saunois et al., 2020), as are ruminant animals (sometimes referred to as walking wetlands). Combustion of organic material during burning will also emit CH_4. Natural reservoirs of old carbon can also release CH_4, such as gas-oil seeps, thawing marine and terrestrial permafrost and mud volcanoes. The total rate of natural CH_4 emissions is thought to be around 218 Tg CH_4 yr^{-1} (based on top-down estimation methods) or 371 Tg CH_4 yr^{-1} (based on bottom-up estimation methods) (Saunois et al., 2020). Humans have added additional CH_4 to this mix through fossil fuel consumption, increased ruminant numbers and expansion of anoxic rice paddies and landfills.

Reconstructing CH_4 levels during the Quaternary

The ancient air trapped in ice cores allows us to directly measure the mixing ratio and isotopic composition of past atmospheric methane. This insight into the response of the methane cycle to external forcing and internal feedbacks of the climate system is extremely valuable, particularly as we look towards the future in a warming world where the potential for methane-climate feedbacks associated with Arctic permafrost degradation and/or tropical wetland emissions could be growing. Methane has also proven to be an excellent proxy for tropical climate variability and a highly useful tool for synchronisation of ice core records at decadal to millennial timescales.

Polar ice core cores provide us with records of past atmospheric methane mixing ratios across the past 800,000 yr. There is no methane proxy measurable in another paleoclimate archive, so we await the retrieval of older ice from Antarctica to extend methane's history further back into the Pleistocene. The temporal resolution of methane mixing ratio records from ice cores can range from around a decade for the youngest Late Holocene air to multiple hundreds of years for the oldest air from deep East Antarctic cores. This variation in temporal resolution is the result of a combination of analytical technique and ice core site conditions (see section 'Preservation of gas signals within ice cores').

Records of past atmospheric methane variations alone do not tell us about the drivers behind those changes. The stable isotopic ratios of carbon ($\delta^{13}C$) and hydrogen (δD) within methane can shed light on relative changes in the strength of the sources. Stable carbon isotope

ratios vary between three broad emissions categories (Sherwood et al., 2017 median values): biogenic (e.g., wetland, ruminants; $\delta^{13}CH_4$ -63 ‰), geologic (e.g., coal, methane hydrates, natural gas seeps; $\delta^{13}CH_4$ -43 ‰) and biomass burning, sometimes called pyrogenic ($\delta^{13}CH_4$ -27 ‰). δD of CH_4 has a similarly depleted signature for biogenic emissions and relatively enriched values for geologic sources and biomass burning. The stable isotope ratios of CH_4 measured on ice core air will always need to be corrected for sink fractionation—when CH_4 is oxidised by OH the remaining air is left isotopically heavier. This effect is much greater for δD than $\delta^{13}CH_4$.

The inter-polar gradient (IPG) between Greenland and Antarctic ice core records can be an informative tool for understanding past changes in the latitudinal distribution of methane sources. Methane levels are higher in the Northern Hemisphere compared to the Southern Hemisphere today and in the past due to the concentration of land-based methane sources in the North. Air is exchanged between hemispheres on a timescale of about a year, meaning that CH_4 variability in both hemispheres is similar—ice core methane records obtained from Greenland or Antarctica should record similar variability. However, the lifetime of methane in the atmosphere is roughly 10 years meaning that CH_4 accumulates in the North and the CH_4 mixing ratio of the Northern Hemisphere is always slightly higher compared to the Southern Hemisphere value.

Analytical Techniques

Over the last decade the measurement of methane mixing ratios in ice cores has been transformed by the introduction of a continuous, online measurement techniques (Chappellaz et al., 2013; Stowasser et al., 2012). The resulting order of magnitude increase in achievable measurement resolution has revealed new abrupt atmospheric methane variations, as well as exposing the presence of low-level production of methane in some settings (see section 'Non-atmospheric CH_4 signals'). In brief, existing Continuous Flow Analysis (CFA) setups are altered so that the gas released from an ice stick melted on a hot plate is extracted from the water stream across a gas-permeable membrane, dried, and injected continuously into a customized laser spectrometer. The low (< 2 mL min^{-1}) flow of gas obtained from CFA requires that the laser spectrometer is operated at a low pressure (typically 20-50 mbar) and the cell volume of the instrument may also be reduced. Sampling frequencies of >1 Hz result in highly precise measurements (± 1 ppb 2σ), reproducible over longer-term intervals (± 1.5 ppb 2σ). As for discrete wet extraction techniques (see below), a correction for under-recovery of CH_4 due to dissolution in the water stream is required and this is achieved via analysis of a simulated gas-water stream using standard gas of known composition (Rhodes et al., 2013).

Traditional 'discrete' techniques use individual ice samples (typically 40-50 g). Gas is usually wet-extracted via melting and refreezing under vacuum (Mitchell et al., 2011) but dry extraction is also possible using a 'cheese grater' apparatus (Etheridge et al., 1998). Gas released is expanded into a sample loop and detection of CH_4 is performed by gas chromatography using a flame-ionisation detector. Long-term precision of ± 1.8 ppb (1σ) can be achieved via this method (Lee et al., 2020b). A new technique that uses sublimation to extract gas that is fed into a laser spectrometer capable of simultaneous measurement of CO_2, CH_4 and N_2O mixing ratios, as well as $\delta^{13}CO_2$, holds great promise for the future (Mächler et al., 2023).

Stable isotopic ratios of methane ($\delta^{13}C$ and δD) are measured by isotope-ratio mass spectrometry after the methane is separated from other gases by gas chromatography and combusted to either CO_2 (for $\delta^{13}C$ analysis) or pyrolized to H_2 (for δD analysis). Care must be taken to avoid analytical bias from krypton interference (Schmitt et al., 2014). Replicate analyses indicate $\delta^{13}C$ measurements are reproducible to within ±0.15 ‰ (1σ) and δD of CH_4 measurements are reproducible to within ±2.3 ‰ (1σ) (Bock et al., 2017).

The ultimate analytical challenge for ice core methane studies is the measurement of the radiocarbon (^{14}C) content of methane, an unambiguous tracer of geologic emissions. This requires huge volumes of ice only obtainable from blue ice zones, such as Taylor Glacier in

Antarctica, where old ice of interest outcrops at the surface. Gas extraction from ~1000 kg (!) of ice per sample is undertaken in the field (Petrenko et al., 2008) and only the air is sent for ^{14}C analysis by Accelerator Mass Spectrometer.

Preservation of gas signals within ice cores

The snow accumulation rate and site temperature at an ice core site are critically important for determining how quickly the gas becomes trapped within the ice and, in turn, this impacts the (1) degree of smoothing of atmospheric variations (hence the temporal resolution of the record) and (2) the phasing between atmospheric composition changes, recorded in the trapped air, and climate signals, recorded in the ice matrix.

Air becomes trapped within air bubbles in the ice once the fresh snow has compacted, sintered, and densified through the firn column. The amount of snow accumulating each year, together with the temperature, control how fast densification and bubble trapping occurs. Typically, air bubbles are closed off by a firn-ice transition depth of 60 to 120 m. Air that is trapped at this depth must always be younger in age than the ice surrounding it and the mean age difference between the ice age and the gas is called the Δage. At a high accumulation location such as Law Dome, Antarctica, Δage can be as low as 30 yr. In contrast, a low accumulation East Antarctic location, such as EPICA Dome C (EDC) may have a Δage of ~2000 yr that increases to >4000 yr in drier glacial periods. Although we can do a good job at calculating Δage by modelling the physics of bubble trapping within firn for the present-day (see Chapter 'Firn Air Processes in Ice Core Science'), it is challenging to achieve for the past when histories of temperature and accumulation rate are more uncertain.

The air is not trapped at 'age zero'. It takes approximately 10 to 100 yr for gas molecules to diffuse through the firn column before they are eventually trapped in bubbles. This process of diffusion leads to mixing of gas within the firn structure, resulting in a smoothed version of atmospheric history being preserved in an ice core. For example, the seasonal cycle in CH_4 mixing ratio present in the atmosphere can never be preserved in an ice core. Additional smoothing is caused by the gradual closure of bubbles over a density range of 0.78-0.84 g cm^{-3}. The mixing of gases within the firn also means that the air that is eventually trapped within an ice layer is not one discrete age but actually a mixture of different ages. The range of ages can be described by the gas age distribution width, which is low at high accumulation sites with relatively fast bubble trapping and much wider at low accumulation sites (or in glacial periods). The consequence of this is that CH_4 records from different ice cores can look slightly different to each other across rapid changes in atmospheric composition. This is nicely illustrated by Spahni et al. (2003) who compare the sharp trough in CH_4 at 8.2 kyr recorded in GRIP with the heavily smoothed version in EDC. Looking forward towards new ice cores currently being drilled at low accumulation rate sites in Antarctica in the search for the 'oldest ice', it is worth noting that firn smoothing may not be as significant as we might expect. Detailed measurements on the Vostok core (Fourteau et al., 2017) suggest a narrower gas air distribution in the Last Glacial relative to what firn transport air models might predict, highlighting that our understanding of firn physics under different climate conditions is limited.

Last 2k

The last 2000 years is fascinating time period for studying the methane cycle because early human activities almost definitely made their mark. These contributions are then completely dwarfed by CH_4 emissions associated with industrialisation in the western world post-1750 CE. The history of atmospheric methane over the last 2000 years is archived in detail by several relatively high accumulation rate ice cores from Greenland and Antarctica (Figure 1). Pre-industrial (pre-1750 CE) methane mixing ratios were around 700 ppb in Antarctica (slightly higher in Greenland) having increased by less than 100 ppb over the previous two millennia. From 1750 CE, CH_4 growth rate increases markedly, further increasing around 1945 CE. By 1948 CE, the age

of the youngest air preserved in air bubbles in the Law Dome Antarctic ice core, the CH_4 level has reached almost 1500 ppb (Etheridge et al., 1998; MacFarling Meure et al., 2006). To take the CH_4 forward in time to the present day, we must sample the air present in the open porosity within the firn column. This allows overlap with methane measurements made on air directly sampled from the atmosphere at Cape Grim and later at South Pole. The excellent match between these measurements—the continuity between ice core air, firn air and directly-sampled air data—is impressive and a testament to the fidelity of the ice core air archive. The post-industrial methane increase is characterised by increases in both $\delta^{13}C$ and δD of CH_4 linked to increasing anthropogenic emissions from agriculture, landfills and fossil fuel extraction relative to the previously dominant natural wetland source (Sowers et al., 2005).

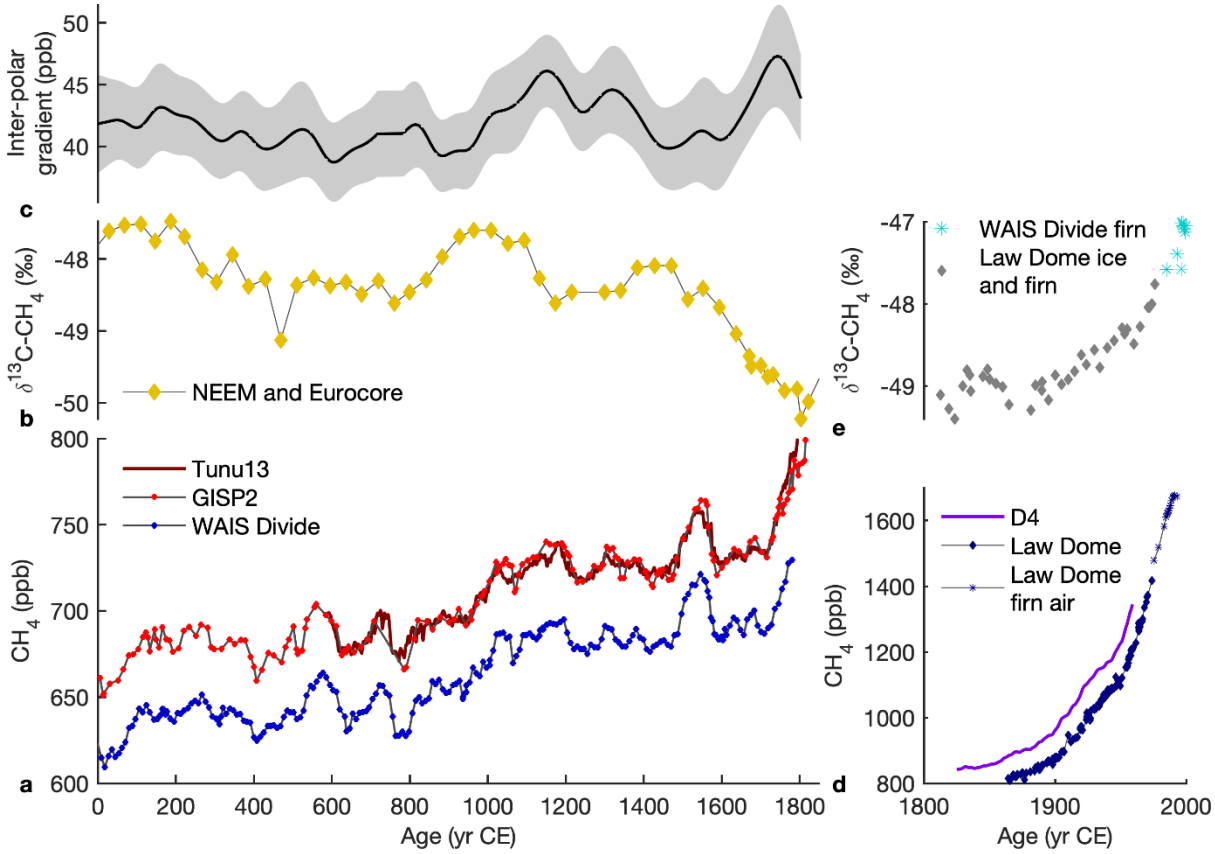

Figure 1: Last two thousand years of methane variability. *(a) CH_4 mixing ratio records from WAIS Divide, Antarctica and GISP2, Greenland (Mitchell et al., 2013) with continuous data from Tunu13 (Rhodes et al., 2016); (b) $\delta^{13}C$ of CH_4 from NEEM and Eurocore (Sapart et al., 2012); (c) Inter-polar gradient between WAIS Divide and GISP2 (Mitchell et al., 2013); (d) Last few hundred years of CH_4 mixing ratio measured on air trapped in bubbles at Law Dome (DE-08 core), CH_4 values measured on DE-08 firn air (Rubino et al., 2019), and continuous CH_4 data from D4 core in Greenland (Rhodes et al., 2016); (e) Recent decades of $\delta^{13}C$ of CH_4 data from WAIS Divide firn (Mischler et al., 2009) and Law Dome ice and firn (Rubino et al., 2019).*

When Ferretti et al. (2005) measured pre-industrial $\delta^{13}CH_4$ values on the Law Dome ice core they expected to measure relatively constant, depleted values consistent with a prevalent wetland source. Instead, they found evidence for human influence on the methane budget of the late pre-industrial Holocene. Together with $\delta^{13}C$ and δD of CH_4 data from the WAIS Divide ice core, a scenario of high biomass burning (enriched isotopic values) prior to 1500 CE followed by

a marked $\delta^{13}CH_4$ decrease of -2 ‰ by 1800 CE emerges. Ferretti et al. argued that the 1800 CE minimum in $\delta^{13}CH_4$ resulted from a significant decrease in biomass burning linked to the colonisation of the Americas and pandemic-related decline of indigenous populations. It seems likely that an increase in CH_4 emissions from ^{13}C-depleted agricultural sources (ruminants, rice paddies) also contributed (Mischler et al., 2009).

The evolution of $\delta^{13}C$ and δD of CH_4 over the late pre-industrial Holocene is not matched by trends in the CH_4 mixing ratio which shows a gradual increase. Sapart et al. (2012) highlight the similarity between the temporal evolution of atmospheric CH_4 and an estimation of land area used by humans as evidence of increasing anthropogenic CH_4 emissions. However, calculation of the IPG between the GISP2 Greenland ice core CH_4 and the WAIS Divide Antarctic ice core CH_4 (Figure 1) reveals no significant trend that might suggest a shift towards Northern regions. Mitchell et al. (2013) conclude that both natural (Southern Hemisphere wetlands) and anthropogenic sources (concentrated in the North) must have contributed to the CH_4 increase.

Multi-decadal variations in methane mixing ratio of up to 55 ppb amplitude are super-imposed on last 2k records from many cores across Greenland and Antarctica (Mitchell et al., 2011; Rhodes et al., 2013). There is no universal explanation for this variability at present. Some features appear to coincide with time periods of war or plague that could plausibly have led to reduced CH_4 emissions but there is also evidence that climate drivers, for example Northern Hemisphere cooling associated with the Little Ice Age, played a role (Mitchell et al., 2011). Recent $\delta^{13}C$ of CH_4 measurements, made at higher resolution and greater precision than previous studies, show three time intervals when $\delta^{13}C$ was enriched for a century or two over the last 2k (Figure 1). These $\delta^{13}C$ excursions do not align with changes in atmospheric CH_4 suggesting that emissions from multiple sources must have changed simultaneously. Source strength reconstructions based on box model inversions suggest that higher biomass burning emissions (with enriched $\delta^{13}C$) were coincident with decreased wetland emissions. The timing of the three $\delta^{13}C$ excursions suggest that natural climatic factors such as the Little Ice Age or Medieval Climate Anomaly, as well as human factors such as the decline of the Roman Empire were likely drivers (Sapart et al., 2012).

Holocene

Several datasets, notably from RICE (Lee et al., 2020a), WAIS Divide (Buizert et al., 2015) and South Pole (Epifanio et al., 2020) ice cores in Antarctica, now extend our record of atmospheric methane variability right through the Holocene at decadal resolution. These records reveal that the multi-decadal variability of the last 2k is a persistent feature of the entire Holocene (Figure 2). Indeed, the WAIS Divide CH_4 record suggests it persists throughout the Last Glacial too. Thus far, ice core gas age scales have been synchronised precisely using this multi-decadal signal, but little work has gone into deciphering its climatic or biogeochemical drivers beyond the suggestion that tropical hydroclimate is involved (Rhodes et al., 2017). A short-lived but distinct trough in CH_4 coincident with the 8.2 ka cooling event across the Northern Hemisphere is resolved in multiple high resolution CH_4 records (Spahni et al., 2003).

Over longer timescales, the ice core record of methane over Holocene can be approximated to a bowl shape (Blunier et al., 1995). Mixing ratios are relatively high (>700 ppb in Antarctica) in the very earliest Holocene and they decrease to a minimum of ~560 ppb by 5 ka (Figure 2), largely following the evolution of Northern Hemisphere (30 °N) insolation. From this point methane mixing ratios increase again towards pre-industrial levels. The departure of CH_4 from the track set by insolation mid-Holocene sets the Holocene apart from other interglacial periods in which CH_4 appears to follow the trend set by NH insolation, presumably due to the influence of local insolation on tropical climate and wetland CH_4 production. This gave rise to the hypothesis that early human activity, specifically expansion of rice paddies across Asia, caused global CH_4 to increase mid-Holocene (Ruddiman, 2003). To counter this argument, Singarayer et al. (2011) proposed a scenario of obliquity-driven strengthening monsoons in the Southern

Hemisphere enhancing natural wetland CH_4 emissions, leading to the observed Late Holocene CH_4 increase.

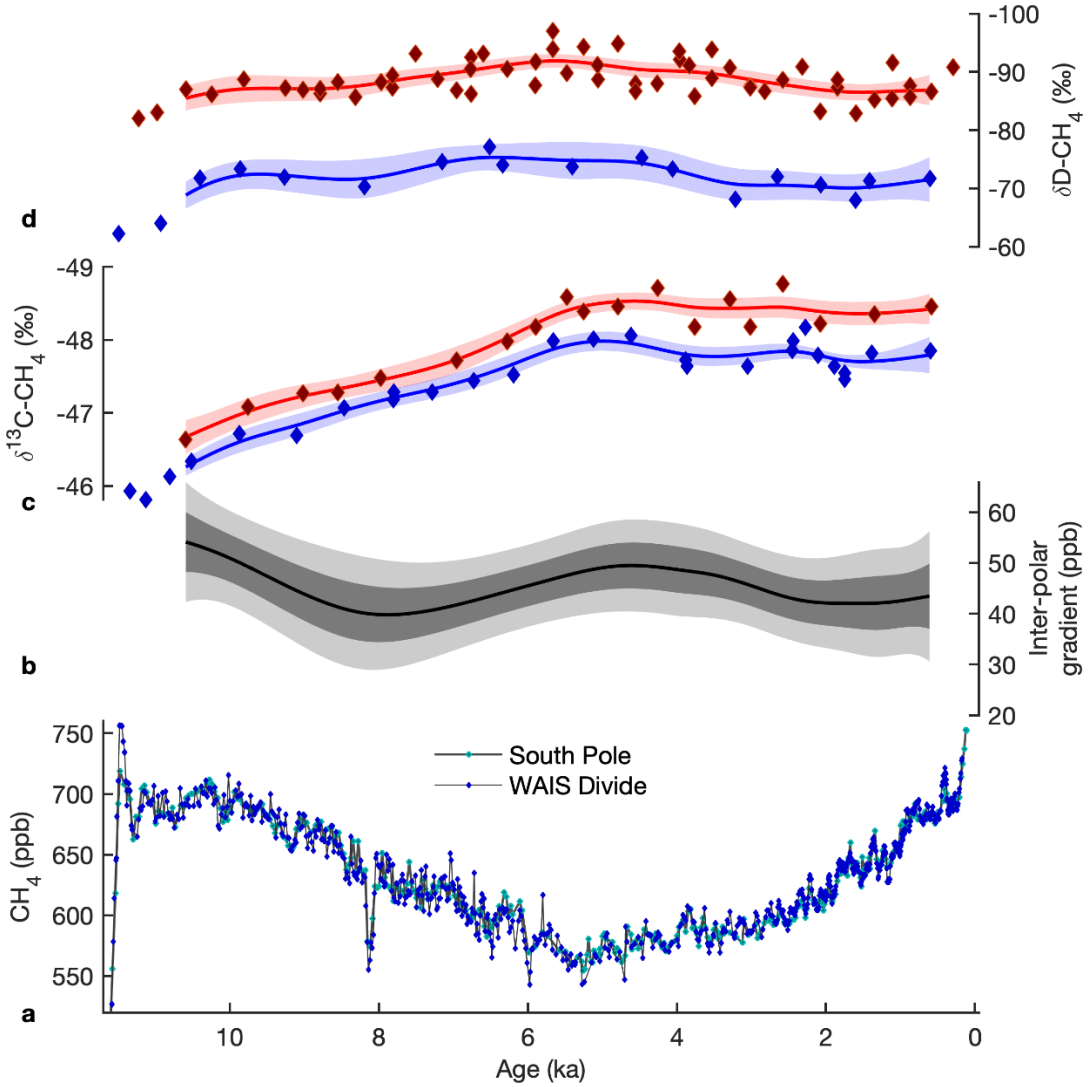

Figure 2: Methane through the Holocene. *(a) CH_4 records from two Antarctic ice cores, South Pole (Epifanio et al., 2020) and WAIS Divide (WAIS Divide Project Members, 2015); (b) CH_4 inter-polar gradient calculated by Beck et al. (2018) from splines fitted to data compiled from multiple ice cores; (c) $\delta^{13}C$ of CH_4 data from Greenland (NGRIP) and Antarctic (EDML, TALDICE) ice cores (diamonds) with splines and their 2σ uncertainty envelopes (Beck et al., 2018); (d) as (c) for δD of CH_4.*

Beck et al. (2018) present the most recent effort at deciphering long-term Holocene CH_4 drivers using CH_4 mixing ratios and stable isotope data from ice cores at both poles input into a 2-box model of the atmosphere. Inversion of the model to obtain CH_4 source histories (assuming constant sink terms) suggests that Southern Hemisphere emissions decreased from 8 ka to 5.5 ka in response to southward migration of the inter-tropical zone (ITCZ). In tandem, the $\delta^{13}C$ signature of the northern CH_4 source decreased by 3 ‰ (Figure 2), which could be attributed to a change in the isotopic signature of the organic precursor material required for CH_4 production, resulting from an increase in the ratio of C3 to C4 plants under rising CO_2 levels, as first suggested by Sowers (2010). Moving into the second half of the Holocene, the isotopic signature of CH_4

emissions did not change (Figure 2) and results suggest the 30 Tg yr^{-1} increase in CH_4 emissions was driven by Southern Hemisphere emissions from wetlands and wildfires. According to Beck et al.'s analysis, Northern Hemisphere CH_4 emissions do not increase until 2000 years ago, inconsistent with an early human influence on the CH_4 cycle.

Last Deglaciation

The methane mixing ratio increased by 340 ppb between the Last Glacial Maximum (LGM, ~20 ka) and the earliest Holocene. This is almost 2.5 times the variation across the entire pre-industrial Holocene and it occurred in several surges rather than as a gradual increase. There are methane records from many ice cores across this interval, the best-resolved being the WAIS Divide continuous record, which is the source of the values quoted here (Rhodes et al., 2015) on the WD2014 timescale (Buizert et al., 2015). Methane begins to increase around 18 ka, very slightly after CO_2 (Marcott et al., 2014), and continues to gradually increase until 14.7 ka when the methane level rises by 160 ppb in 200 years. Methane remains relatively high, but oscillating through a >100 ppb range, until the mixing ratio abruptly decreases by 146 ppb at 12.8 ka and remains low until the fastest transition recorded in the WAIS Divide core, a 6 ppb yr^{-1} increase at 11.6 ka to early Holocene values.

Methane clearly follows Greenland ice core $\delta^{18}O$ across this sequence and we can assign the name tags of Heinrich Stadial 1, Bølling-Allerød and Younger Dryas to the time intervals described above (Figure 3). There are essentially two possible explanations for the remarkable similarity of methane and Greenland $\delta^{18}O$ across the deglaciation: (1) high latitude Northern Hemisphere climate controls CH_4 emissions from boreal wetland and permafrost regions, (2) high latitude Northern Hemisphere climate modulates tropical hydroclimate, which in turn impacts CH_4 emissions from tropical wetlands. The IPG should be a useful tool to distinguish between these scenarios but, until very recently, some Greenland CH_4 measurements were biased very slightly high in dust-rich samples (see section 'Non atmospheric CH_4 signals'). A recent study presents a revised IPG across the deglaciation using Greenland CH_4 corrected for this excess CH_4 (Figure 3) and suggests that tropical sources were responsible for the majority of the methane variation (Riddell-Young et al., 2023). From ~16 ka, there is evidence for extra-tropical emissions, likely boreal wetland expansion and/or permafrost degradation, which are responsible for 45% total of the total CH_4 increase across the deglaciation.

The phasing of the abrupt methane increases relative to the Greenland warmings can be precisely estimated using isotopic measurements on nitrogen present in the ice core air. The ratio of ^{15}N to ^{14}N increases sharply in response to abrupt warming at the ice sheet surface because of thermal fractionation during diffusion of N_2 through the firn (see Chapter 'Firn Air Processes in Ice Core Science'). The first study to apply this method found that CH_4 began to increase 20-30 years after the onset of Greenland warming into the Bølling-Allerød (Severinghaus, 1999). A more recent study, with improved uncertainty accounting, concluded that the methane increase and Greenland warming were essentially synchronous (Greenland temperature leading by 4.5 +21 -24 years) (Rosen et al., 2014). This suggests that climate signals are quickly transmitted between the high latitudes and the tropics via an atmospheric teleconnection.

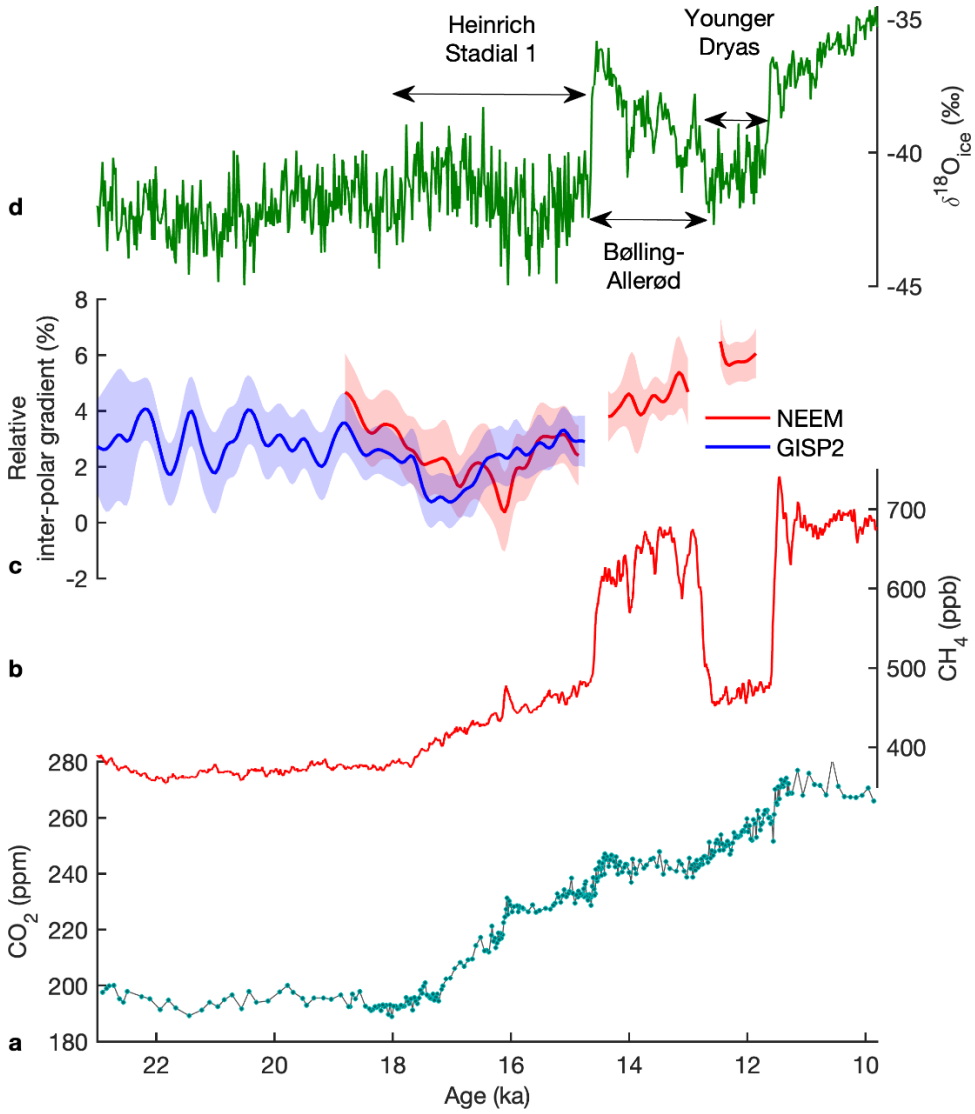

Figure 3: Methane across the deglaciation. *(a) CO_2 mixing ratio record from WAIS Divide (Marcott et al., 2014); (b) CH_4 mixing ratio measured continuously, also from WAIS Divide (Rhodes et al., 2015); (c) Relative inter-polar gradient (([Greenland CH_4/Antarctic CH_4]-1)*100) calculated from comparison between CH_4 data from WAIS Divide and NEEM (blue) or GISP2 (red) plotted with 95% confidence intervals (Riddell-Young et al., 2023). A shift towards more positive values indicates a net northward shift in CH_4 source region latitude. (d) $\delta^{18}O$ of ice record from NGRIP, Greenland (Svensson et al., 2008).*

Last Glacial

In comparison to the Holocene, ice core methane records through the Last Glacial period are very dynamic, varying by up to 200 ppb in a matter of centuries, in sync with the repeated abrupt warming followed by gradual cooling of the Dansgaard-Oeschger (DO) cycles recorded by Greenland ice core $\delta^{18}O$ (Figure 4) (Brook et al., 1996; Rhodes et al., 2015). Here again, $\delta^{15}N$ measurements demonstrate tight phasing (within decades) between Greenland warming and CH_4 increase across each of the abrupt transitions (Baumgartner et al., 2014). Reliable IPG data currently only extend back to 27.5 ka, but suggest that tropical sources dominated the Last Glacial methane budget to this point (Riddell-Young et al., 2023). If we consider that much of the boreal Northern Hemisphere was covered by ice sheet or frozen permafrost, it seems at least likely that this remained the case for the majority of the Last Glacial.

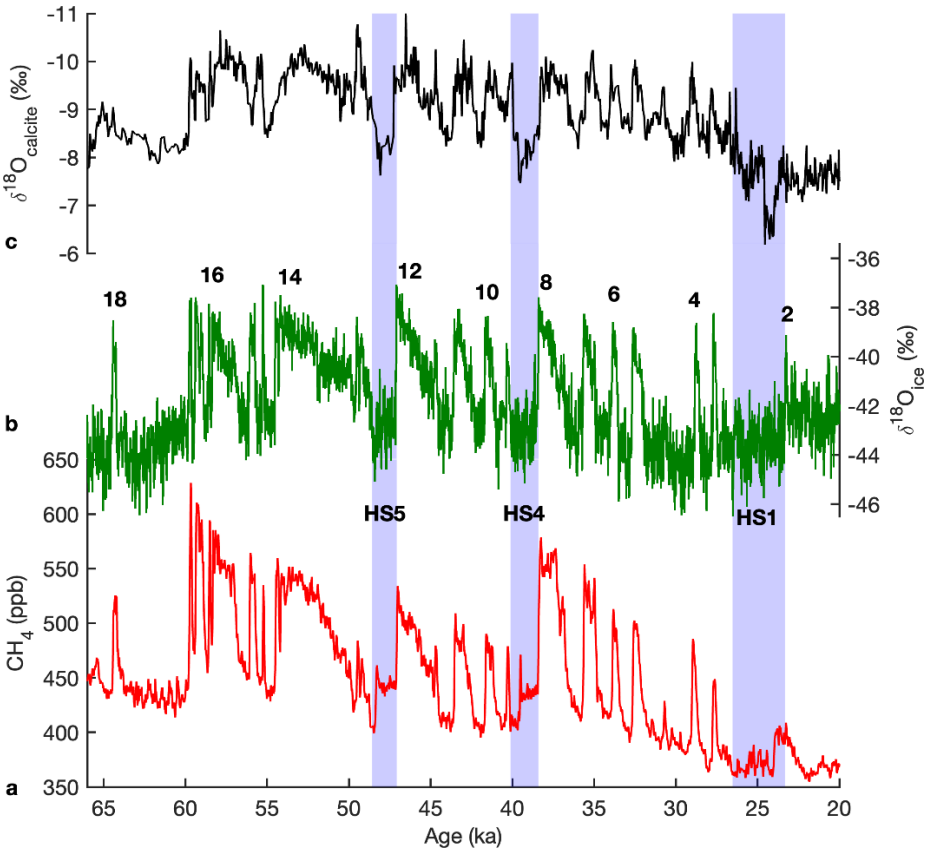

Figure 4: Abrupt millennial scale variations in methane and climate during the Last Glacial. *(a) WAIS Divide CH_4 (Rhodes et al., 2015); (b) $\delta^{18}O$ of ice record from NGRIP, Greenland (Svensson et al., 2008); (c) composite of Asian speleothem $\delta^{18}O$ of calcite records, a proxy for Asian Monsoon strength (Cheng et al., 2016). Selected DO events are numbered and Heinrich Stadials (HS) containing CH_4 increases with no equivalent change in Greenland $\delta^{18}O$ are shaded blue.*

Explaining the large and rapid oscillations in CH_4 associated with DO climate variability therefore requires that tropical CH_4 sources, predominantly wetlands but also biomass burning, were incredibly dynamic and responsive to Arctic climate change. Other high resolution paleoclimate archives provide abundant evidence for tropical climate change on millennial time scales, particularly changes to precipitation patterns that closely control wetland CH_4 production. For example, the Hulu cave speleothem $\delta^{18}O$ record (East China) closely corresponds to Greenland ice core $\delta^{18}O$ and CH_4, showing enriched $\delta^{18}O$ in stadials (cool stages of DO events) and depleted $\delta^{18}O$ in interstadials (warm stages of DO events) (Cheng et al., 2016) (Figure 4). The controls on speleothem $\delta^{18}O$ are complex but to first-order this indicates a stronger East Asian monsoon in interstadials and a relatively weak East Asian monsoon in stadials. A similar pattern of alternating climate conditions between wet interstadials and drier stadials is recorded in the sediments of Cariaco Basin (off north coast of Venezuela) and the Arabian Sea (Deplazes et al., 2013). Southern Hemisphere proxy records tell the opposite story—the Pacupahuain Cave speleothem (Peru) $\delta^{18}O$ record suggests dry interstadials and wet stadials (Kanner et al., 2012). Taken together, the proxy data support a scenario in which high latitude climate change results in an imbalance of heat between the hemispheres impacting the mean latitudinal position, and likely also the seasonal range, of the major tropical rainbelts linked to the ITCZ and monsoonal systems (Chiang et al., 2008).

Numerical models that couple DO-like climate simulations to process-bases wetland emission models have so far found it difficult to reproduce the large change in tropical wetland CH_4 emissions (~60 Tg yr^{-1}) required to match the CH_4 mixing ratio shifts recorded by ice cores

(Hopcroft et al., 2011; Ringeval et al., 2013). Part of the problem might lie in the models themselves, which typically have trouble simulating the ITCZ accurately and show widely different performance at simulating present-day wetland CH_4 emissions (Melton et al., 2013). Alternatively, another CH_4 source may be required to explain the large CH_4 increases associated with some DO events.

Carbon isotopes of methane ($\delta^{13}C$) measured in detail across DO events in the Vostok and EDML Antarctic ice cores reveal some extraordinary features (Möller et al., 2013). $\delta^{13}CH_4$ and CH_4 vary independently through the Last Glacial. When CH_4 levels increase sharply at the onset of DO events, $\delta^{13}CH_4$ shows no equivalent abrupt change. This suggests that any increase in the strength of emissions from tropical CH_4 wetlands has to be matched by a proportional rise in biomass burning emissions, in order to maintain the $\delta^{13}CH_4$ signature. $\delta^{13}CH_4$ is not constant through the Last Glacial though. In fact, $\delta^{13}CH_4$ appears to co-vary with the CO_2 mixing ratio on millennial timescales. Möller et al. (2013) speculate that this results from changing $\delta^{13}C$ of the organic material decomposed in wetland ecosystems, maybe via the influence of CO_2 on the C3/C4 plant ratio.

An alternative potential mechanism of releasing lots of CH_4 quickly into the atmosphere in near-synchroneity with Arctic warming is the rapid release of old, stored carbon. While researchers in the early 1990s were focused on methane clathrates ('the clathrate gun hypothesis'), the focus has shifted more recently to also consider permafrost degradation and thermokarst lake formation (associated with permafrost thaw). It is difficult to disentangle CH_4 contributions from these old carbon (geologic) sources from biomass burning emissions using $\delta^{13}C$ and δD of CH_4 because both sources are enriched relative to the dominant wetland source. Measurement of the radiocarbon (^{14}C) content of CH_4 provides an unambiguous tool to distinguish contemporary CH_4 sources (wetlands or biomass burning) from old, geologic CH_4 sources. Essentially, methane released from old carbon sources will be ^{14}C-dead (^{14}C-CH_4 = 0‰) while the ^{14}C of CH_4 released effectively instantaneously by wetlands or biomass burning will reflect the ^{14}C of the atmospheric CO_2 from which the plant-matter precursor was formed. Measurements of $\Delta^{14}CH_4$ across the two prominent CH_4 increases of the last deglaciation, the transition into the Bolling-Allerod (14.6–14.45 ka) and the transition from the Younger Dryas into the earliest Holocene (11.7–11.3 ka) show no evidence of contribution from old carbon reservoirs (Dyonisius et al., 2020). The $\Delta^{14}CH_4$ values match those of the contemporaneous atmosphere (the IntCal13 radiocarbon curve), consistent with CH_4 emissions from wetlands and biomass burning.

Methane closely resembles Greenland $\delta^{18}O$ for most of the Last Glacial but not quite all of it. Abrupt CH_4 increases with no corresponding change in Greenland $\delta^{18}O$ are found in four stadial intervals (Figure 4, 3 shown). All are Heinrich Stadials—stadials when Heinrich events occurred, massive iceberg armadas originating from the Laurentide ice sheet. Although the Greenland temperature doesn't appear to be sensitive to these events (Martin et al., 2023), Heinrich events impacted climate widely, displacing the ITCZ southward (Pedro et al., 2018), as reflected by signals of extreme drying recorded in the Hulu cave speleothem and signs of strong monsoons recorded in South America. Rhodes et al. (2015) link the CH_4 increases directly to onset of Heinrich events, proposing that the extreme cooling at northern high latitudes forced concentration of tropical rainbelts in the southern tropics, increasing wetland CH_4 production there.

Last eight glacial-interglacial cycles

Deep East Antarctic ice cores from Vostok, EDC and Dome Fuji have all yielded methane records spanning several glacial-interglacial cycles. The Vostok record covers the last 420,000 years and reveals that CH_4 levels fluctuated between interglacial values around 800 ppb and glacial values around 320 ppb (Petit et al., 1999). Extension of the CH_4 record back to 800 ka via the EDC ice core definitively shows that our current >1900 ppb atmospheric methane is unprecedented

within the last eight glacial-interglacial cycles (Loulergue et al., 2008) (Figure 5). Methane's direct contribution to radiative forcing changes across glacial-interglacial cycles is relatively minor compared to CO_2, and similar to nitrous oxide (N_2O). Together, CH_4 and N_2O account for ~20% of the total greenhouse gas forcing (Schilt et al., 2010b).

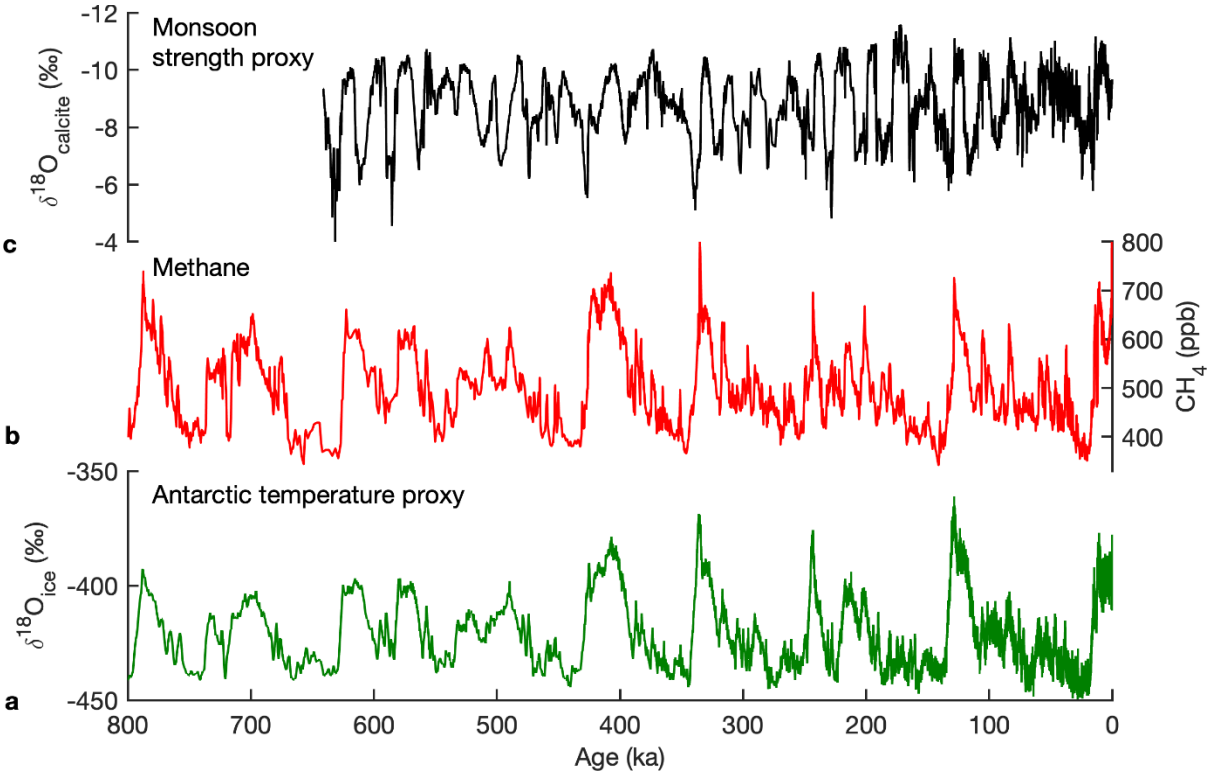

Figure 5: *Glacial-interglacial cycles in methane. EDC CH_4 record (b, Loulergue et al. 2008) with $\delta^{18}O$ of ice from EDC (a, Jouzel et al. 2007), a proxy for site temperature, and a composite of Asian speleothem $\delta^{18}O$ of calcite records, a proxy for Asian Monsoon strength (c, Cheng et al. 2016).*

The EDC $\delta^{18}O$ of ice record, representing Antarctic temperature, shows that interglacials prior to 430 ka were cooler than those that occurred later (EPICA community members, 2004), an apparent transition referred to as the Mid-Brunhes Event (MBE) (Yin, 2013). CO_2 appears to follow this trend but for CH_4 the distinction between pre- and post-MBE is less clear-cut (Figure 5). With the exception of MIS 19, the earlier interglacials do appear to have lower CH_4 maxima but comparison of the mean interglacial CH_4 reveals no significant difference (Schilt et al., 2010a). Spectral analysis of the EDC CH_4 record reveals a strong 100 kyr component, as we might expect, but its power is decreased post-MBE, with precession frequencies becoming stronger. Comparison of CH_4 to the $\delta^{18}O$ signal from a composite of Chinese speleothems, a proxy for monsoon strength (Cheng et al., 2016), highlights a common precessional frequency pattern, periodicity similar to the precessional cycle of the Earth, roughly 23,000 years (Figure 5). All deglaciations exhibit a similar two-step increase in CH_4: an initially slow rise over a few millennia is followed by a rapid increase over one to three centuries. The short-lived reversal in CH_4 across the Younger Dryas (Figure 3) appears to be unique to the most recent deglaciation.

Methane isotope data ($\delta^{13}C$ and δD) measured on Antarctic ice cores across several glacial-interglacial cycles indicate a dominant role for tropical wetland methane emissions, modulated by tropical hydroclimate, i.e., monsoon strength, in orbital scale variability in atmospheric methane (Bock et al., 2017). A contribution from a changing sink strength, maybe

due to changes OH levels in the tropics cannot be ruled out, although modelling work examining the last deglaciation argues against it (Levine et al., 2011). It is also likely that a portion of the elevated CH_4 levels of interglacials was sourced from boreal wetlands of the Northern Hemisphere that were exposed, wetted and warmed by retreating ice sheets.

The long methane records of Vostok and EDC reveal that millennial scale abrupt CH_4 variations are a persistent feature of glacial conditions. CH_4 variability similar to that associated with the Dansgaard-Oeschger events of the Last Glacial is observed in multiple glacial periods. As Greenland ice cores do not extend beyond the Last Interglacial, CH_4 offers an opportunity to reconstruct Greenland temperature but accurately pinning down the phasing of CH_4 relative to Antarctic temperature (δD) is difficult due to the relatively large Δage of these cores (Delmotte et al., 2004). Still, the presence of millennial scale variability in CH_4, associated with Antarctic δD variability equivalent to AIM events, strongly suggests that the mechanisms of abrupt climate change over these timescales were in operation throughout the previous eight glacial-interglacial cycles.

Non-atmospheric CH_4 signals

Methane measurements on air extracted from tropical glaciers in the early 2000s revealed local artifacts of non-atmospheric origin (Campen et al., 2003). These could only partially be explained by the effect of seasonal melt and meltwater percolation impacting the solubility of gases in the ice layers as they refreeze, suggesting CH_4 production within the ice sheet (in situ) may be operating. A CH_4 record measured on a Himalayan ice core is similarly impacted but application of a filter to remove implausibly high frequency oscillations (that would not have survived firn-based gas record smoothing) allowed an attempt at paleo-atmospheric reconstruction (Hou et al., 2013). In Greenland ice, narrow, isolated layers of elevated CH_4 (by 35–80 ppb) in the Late Holocene continuous CH_4 record NEEM (Rhodes et al., 2013) also suggests potential in situ CH_4 production, although subsequent measurements on three other Greenland cores only found similar signals associated with melt layers (Rhodes et al., 2016).

Careful inspection of CH_4 data from Greenland Last Glacial ice identified a systematic positive (30–40 ppb) offset in CH_4, measured using discrete wet extraction methods, in dust-rich ice layers (Lee et al., 2020b). Investigation into the stable isotopic composition of excess CH_4 and associated trace gas signatures suggests that abiotic decomposition of organic matter is the most likely production mechanism (Mühl et al., 2023). This excess CH_4 must corrected for before accurate calculation of the CH_4 inter-polar gradient (see section 'Last Deglaciation') and imparts a significant bias on the stable isotopic composition of CH_4, calling into question some previously published Greenland ice core data.

A second type of non-atmospheric CH_4 signal observed in ice cores is the trapping signal—the seasonal variation in CH_4 mixing ratio between adjacent summer and winter ice layers during time periods of rapid CH_4 growth rate. This phenomenon was first observed in Law Dome ice (Etheridge et al., 1992) and then reported in Holocene WAIS Divide firn and Greenland ice (Mitchell et al., 2015; Rhodes et al., 2016). The seasonal oscillations are not a reflection of the seasonal cycle of atmospheric CH_4 but a product of the staggered timing of bubble closure between adjacent ice layers of different physical properties. Fourteau et al. (2017) also report trapping signal artifacts, this time not annual, across rapid DO event transitions in Vostok ice, highlighting the benefit of high resolution CH_4 measurements at low accumulation ice core sites.

Future outlook

As the international ice core community strives to retrieve the oldest continuous ice cores yet from Antarctica, we look forward to new records of methane and other greenhouse gases than span the enigmatic Mid-Pleistocene Transition. How did methane variability change as glacial-interglacial cycles switched from ~41 kyr to ~100 kyr and global ice volume increased? We will soon know.

There is also a lot to be learned from the very youngest ice core gas available to us. The uncertainties on the present-day methane budget could be narrowed down with a better understanding of source and sink behaviour in the last few centuries. For example, measurements of the radiocarbon content of carbon monoxide have the potential to reconstruct past variation in atmospheric OH, the major sink of atmospheric CH_4.

As we look towards our future in a warming world, we should be concerned about the potential for unexpected methane-climate feedbacks. Ice core methane records clearly show us that past rapid warming of the high northern latitudes caused huge increases in tropical wetland emissions for example (Nisbet et al., 2023). Closer collaboration between the ice core community, atmospheric scientists studying the present-day atmosphere and climate-chemistry modellers is becoming more important as the Earth System Models used for climate projections are augmented to include key biogeochemical processes (Folberth et al., 2022).

References

Arias, P.A., Bellouin, N., Jones, R.G., Naik, V., Plattner, G.-K., Rogelj, J., Sillmann, J., Storelvmo, T., Thorne, P.W., Trewin, B., Rao, K.A., Adhikary, B., Allan, R.P., Armour, K., Barimalala, R., Canadell, J.G., Cassou, C., Cherchi, A., Collins, W., Corti, S., Cruz, F., Dentener, F.J., Dereczynski, C., Luca, A.D., Diongue, A., Doblas-Reyes, F.J., Dosio, A., Douville, H., Engelbrecht, F., Fyfe, J.C., Gillett, N.P., Goldfarb, L., 2021. Technical Summary. IPCC Working Group 1 112.

Baumgartner, M., Kindler, P., Eicher, O., Floch, G., Schilt, A., Schwander, J., Spahni, R., Capron, E., Chappellaz, J., Leuenberger, M., Fischer, H., Stocker, T.F., 2014. NGRIP CH4 concentration from 120 to 10 kyr before present and its relation to a δ15N temperature reconstruction from the same ice core. Clim. Past 10, 903–920. https://doi.org/10.5194/cp-10-903-2014

Beck, J., Bock, M., Schmitt, J., Seth, B., Blunier, T., Fischer, H., 2018. Bipolar carbon and hydrogen isotope constraints on the Holocene methane budget. Biogeosciences 15, 7155–7175. https://doi.org/10.5194/bg-15-7155-2018

Blunier, T., Chappellaz, J., Schwander, J., Stauffer, B., Raynaud, D., 1995. Variations in atmospheric methane concentration during the Holocene epoch. Nature 374, 46–49.

Bock, M., Schmitt, J., Beck, J., Seth, B., Chappellaz, J., Fischer, H., 2017. Glacial/interglacial wetland, biomass burning, and geologic methane emissions constrained by dual stable isotopic CH4 ice core records. PNAS 114, E5778–E5786. https://doi.org/10.1073/pnas.1613883114

Brook, E.J., Sowers, T., Orchardo, J., 1996. Rapid variations in atmospheric methane concentration during the past 110,000 years. Science 273, 1087–1091.

Buizert, C., Cuffey, K.M., Severinghaus, J.P., Baggenstos, D., Fudge, T.J., Steig, E.J., Markle, B.R., Winstrup, M., Rhodes, R.H., Brook, E.J., Sowers, T.A., Clow, G.D., Cheng, H., Edwards, R.L., Sigl, M., McConnell, J.R., Taylor, K.C., 2015. The WAIS Divide deep ice core WD2014 chronology – Part 1: Methane synchronization (68–31 ka BP) and the gas age–ice age difference. Clim. Past 11, 153–173. https://doi.org/10.5194/cp-11-153-2015

Campen, R.K., Sowers, T., Alley, R.B., 2003. Evidence of microbial consortia metabolizing within a low-latitude mountain glacier. Geology 31, 231–234. https://doi.org/10.1130/0091-7613

Chappellaz, J., Stowasser, C., Blunier, T., Baslev-Clausen, D., Brook, E.J., Dallmayr, R., Faïn, X., Lee, J.E., Mitchell, L.E., Pascual, O., Romanini, D., Rosen, J., Schüpbach, S., 2013. High-resolution glacial and deglacial record of atmospheric methane by continuous-flow and laser spectrometer analysis along the NEEM ice core. Clim. Past 9, 2579–2593. https://doi.org/10.5194/cp-9-2579-2013

Cheng, H., Edwards, R.L., Sinha, A., Spötl, C., Yi, L., Chen, S., Kelly, M., Kathayat, G., Wang, X., Li, X., Kong, X., Wang, Y., Ning, Y., Zhang, H., 2016. The Asian monsoon over the past 640,000 years and ice age terminations. Nature 534, 640–646. https://doi.org/10.1038/nature18591

Chiang, J.C.H., Cheng, W., Bitz, C.M., 2008. Fast teleconnections to the tropical Atlantic sector from Atlantic thermohaline adjustment. Geophys. Res. Lett. 35, L07704. https://doi.org/10.1029/2008GL033292

Delmotte, M., Chappellaz, J., Brook, E., Yiou, P., Barnola, J.M., Goujon, C., Raynaud, D., Lipenkov, V.I., 2004. Atmospheric methane during the last four glacial-interglacial cycles: Rapid changes and

their link with Antarctic temperature. Journal of Geophysical Research: Atmospheres 109. https://doi.org/10.1029/2003JD004417

Deplazes, G., Luckge, A., Peterson, L.C., Timmermann, A., Hamann, Y., Hughen, K.A., Rohl, U., Laj, C., Cane, M.A., Sigman, D.M., Haug, G.H., 2013. Links between tropical rainfall and North Atlantic climate during the last glacial period. Nature Geosci 6, 213–217.

Dyonisius, M.N., Petrenko, V.V., Smith, A.M., Hua, Q., Yang, B., Schmitt, J., Beck, J., Seth, B., Bock, M., Hmiel, B., Vimont, I., Menking, J.A., Shackleton, S.A., Baggenstos, D., Bauska, T.K., Rhodes, R.H., Sperlich, P., Beaudette, R., Harth, C., Kalk, M., Brook, E.J., Fischer, H., Severinghaus, J.P., Weiss, R.F., 2020. Old carbon reservoirs were not important in the deglacial methane budget. Science 367, 907–910. https://doi.org/10.1126/science.aax0504

EPICA community members, 2004. Eight glacial cycles from an Antarctic ice core. Nature 429, 623–628. https://doi.org/10.1038/nature02599

Epifanio, J.A., Brook, E.J., Buizert, C., Edwards, J.S., Sowers, T.A., Kahle, E.C., Severinghaus, J.P., Steig, E.J., Winski, D.A., Osterberg, E.C., Fudge, T.J., Aydin, M., Hood, E., Kalk, M., Kreutz, K.J., Ferris, D.G., Kennedy, J.A., 2020. The SP19 chronology for the South Pole Ice Core – Part 2: gas chronology, Δage, and smoothing of atmospheric records. Climate of the Past 16, 2431–2444. https://doi.org/10.5194/cp-16-2431-2020

Etheridge, D., Pearman, G.I., Fraser, P.J., 1992. Changes in tropospheric methane between 1841 and 1978 from a high accumulation-rate Antarctic ice core. Tellus 44B, 282–294.

Etheridge, D.M., Steele, L.P., Francey, R.J., Langenfelds, R.L., 1998. Atmospheric methane between 1000 AD and present: Evidence of anthropogenic emissions and climatic variability. Journal of Geophysical Research 103, 15979–15993. https://doi.org/10.1029/98JD00923

Ferretti, D.F., Miller, J.B., White, J.W.C., Etheridge, D.M., Lassey, K.R., Lowe, D.C., Meure, C.M.M., Dreier, M.F., Trudinger, C.M., Ommen, T.D. van, Langenfelds, R.L., 2005. Unexpected Changes to the Global Methane Budget over the Past 2000 Years. Science 309, 1714–1717. https://doi.org/10.1126/science.1115193

Folberth, G.A., Staniaszek, Z., Archibald, A.T., Gedney, N., Griffiths, P.T., Jones, C.D., O'Connor, F.M., Parker, R.J., Sellar, A.A., Wiltshire, A., 2022. Description and Evaluation of an Emission-Driven and Fully Coupled Methane Cycle in UKESM1. J Adv Model Earth Syst 14. https://doi.org/10.1029/2021MS002982

Fourteau, K., Faïn, X., Martinerie, P., Landais, A., Ekaykin, A.A., Lipenkov, V.Ya., Chappellaz, J., 2017. Analytical constraints on layered gas trapping and smoothing of atmospheric variability in ice under low-accumulation conditions. Clim. Past 13, 1815–1830. https://doi.org/10.5194/cp-13-1815-2017

Hopcroft, P.O., Valdes, P.J., Beerling, D.J., 2011. Simulating idealized Dansgaard-Oeschger events and their potential impacts on the global methane cycle. Quaternary Science Reviews 30, 3258–3268. https://doi.org/10.1016/j.quascirev.2011.08.012

Hou, S., Chappellaz, J., Raynaud, D., Masson-Delmotte, V., Jouzel, J., Bousquet, P., Hauglustaine, D., 2013. A new Himalayan ice core CH4 record: possible hints at the preindustrial latitudinal gradient. Climate of the Past 9, 2549–2554. https://doi.org/10.5194/cp-9-2549-2013

Jouzel, J., Masson-Delmotte, V., Cattani, O., Dreyfus, G., Falourd, S., Hoffmann, G., Minster, B., Nouet, J., Barnola, J.M., Chappellaz, J., Fischer, H., Gallet, J.C., Johnsen, S., Leuenberger, M., Loulergue, L., Luethi, D., Oerter, H., Parrenin, F., Raisbeck, G., Raynaud, D., Schilt, A., Schwander, J., Selmo, E., Souchez, R., Spahni, R., Stauffer, B., Steffensen, J.P., Stenni, B., Stocker, T.F., Tison, J.L., Werner, M., Wolff, E.W., 2007. Orbital and Millennial Antarctic Climate Variability over the Past 800,000 Years. Science 317, 793–796. https://doi.org/10.1126/science.1141038

Kanner, L.C., Burns, S.J., Cheng, H., Edwards, R.L., 2012. High-latitude forcing of the South American summer monsoon during the Last Glacial. Science 335, 570–573. https://doi.org/10.1126/science.1213397

Lee, J.E., Brook, E.J., Bertler, N.A.N., Buizert, C., Baisden, T., Blunier, T., Ciobanu, V.G., Conway, H., Dahl-Jensen, D., Fudge, T.J., Hindmarsh, R., Keller, E.D., Parrenin, F., Severinghaus, J.P., Vallelonga, P., Waddington, E.D., Winstrup, M., 2020a. An 83 000-year-old ice core from Roosevelt Island, Ross Sea, Antarctica. Climate of the Past 16, 1691–1713. https://doi.org/10.5194/cp-16-1691-2020

Lee, J.E., Edwards, J.S., Schmitt, J., Fischer, H., Bock, M., Brook, E.J., 2020b. Excess methane in Greenland ice cores associated with high dust concentrations. Geochimica et Cosmochimica Acta 270, 409–430. https://doi.org/10.1016/j.gca.2019.11.020

Levine, J.G., Wolff, E.W., Hopcroft, P.O., Valdes, P.J., 2012. Controls on the tropospheric oxidizing capacity during an idealized Dansgaard-Oeschger event, and their implications for the rapid rises in atmospheric methane during the last glacial period. Geophysical Research Letters 39. https://doi.org/10.1029/2012gl051866

Levine, J.G., Wolff, E.W., Jones, A.E., Sime, L.C., Valdes, P.J., Archibald, A.T., Carver, G.D., Warwick, N.J., Pyle, J.A., 2011. Reconciling the changes in atmospheric methane sources and sinks between the Last Glacial Maximum and the pre-industrial era. Geophysical Research Letters 38. https://doi.org/10.1029/2011GL049545

Loulergue, L., Schilt, A., Spahni, R., Masson-Delmotte, V., Blunier, T., Lemieux, B., Barnola, J.M., Raynaud, D., Stocker, T.F., Chappellaz, J., 2008. Orbital and millennial-scale features of atmospheric CH4 over the past 800,000 years. Nature 453, 383–6. https://doi.org/10.1038/nature06950

MacFarling Meure, C., Etheridge, D., Trudinger, C., Steele, P., Langenfelds, R., van Ommen, T., Smith, A., Elkins, J., 2006. Law Dome CO2, CH4 and N2O ice core records extended to 2000 years BP. Geophysical Research Letters 33, doi:10.1029/2006GL026152.

Mächler, L., Baggenstos, D., Krauss, F., Schmitt, J., Bereiter, B., Walther, R., Reinhard, C., Tuzson, B., Emmenegger, L., Fischer, H., 2023. Laser-induced sublimation extraction for centimeter-resolution multi-species greenhouse gas analysis on ice cores. Atmospheric Measurement Techniques 16, 355–372. https://doi.org/10.5194/amt-16-355-2023

Marcott, S.A., Bauska, T.K., Buizert, C., Steig, E.J., Rosen, J.L., Cuffey, K.M., Fudge, T.J., Severinghaus, J.P., Ahn, J., Kalk, M.L., McConnell, J.R., Sowers, T., Taylor, K.C., White, J.W.C., Brook, E.J., 2014. Centennial-scale changes in the global carbon cycle during the last deglaciation. Nature 514, 616–619. https://doi.org/10.1038/nature13799

Martin, K.C., Buizert, C., Edwards, J.S., Kalk, M.L., Riddell-Young, B., Brook, E.J., Beaudette, R., Severinghaus, J.P., Sowers, T.A., 2023. Bipolar impact and phasing of Heinrich-type climate variability. Nature 617, 100–104. https://doi.org/10.1038/s41586-023-05875-2

Melton, J.R., Wania, R., Hodson, E.L., Poulter, B., Ringeval, B., Spahni, R., Bohn, T., Avis, C.A., Beerling, D.J., Chen, G., Eliseev, A.V., Denisov, S.N., Hopcroft, P.O., Lettenmaier, D.P., Riley, W.J., Singarayer, J.S., Subin, Z.M., Tian, H., Zürcher, S., Brovkin, V., van Bodegom, P.M., Kleinen, T., Yu, Z.C., Kaplan, J.O., 2013. Present state of global wetland extent and wetland methane modelling: conclusions from a model inter-comparison project (WETCHIMP). Biogeosciences 10, 753–788. https://doi.org/10.5194/bg-10-753-2013

Mischler, J.A., Sowers, T.A., Alley, R.B., Battle, M., McConnell, J.R., Mitchell, L., Popp, T., Sofen, E., Spencer, M.K., 2009. Carbon and hydrogen isotopic composition of methane over the last 1000 years. Global Biogeochem. Cycles 23, GB4024. https://doi.org/10.1029/2009GB003460

Mitchell, L., Brook, E., Lee, J.E., Buizert, C., Sowers, T., 2013. Constraints on the Late Holocene anthropogenic contribution to the atmospheric methane budget. Science 342, 964–966. https://doi.org/10.1126/science.1238920

Mitchell, L.E., Brook, E.J., Sowers, T., McConnell, J.R., Taylor, K., 2011. Multidecadal variability of atmospheric methane, 1000-1800 C.E. Journal of Geophysical Research 116, doi:10.1029/2010JG001441. https://doi.org/10.1029/2010jg001441

Mitchell, L.E., Buizert, C., Brook, E.J., Breton, D.J., Fegyveresi, J., Baggenstos, D., Orsi, A., Severinghaus, J., Alley, R.B., Albert, M., Rhodes, R.H., McConnell, J.R., Sigl, M., Maselli, O., Gregory, S., Ahn, J., 2015. Observing and modeling the influence of layering on bubble trapping in polar firn. Journal of Geophysical Research: Atmospheres 120, 2558–2574. https://doi.org/10.1002/2014JD022766

Möller, L., Sowers, T., Bock, M., Spahni, R., Behrens, M., Schmitt, J., Miller, H., Fischer, H., 2013. Independent variations of CH4 emissions and isotopic composition over the past 160,000 years. Nature Geoscience 6, 885–890. https://doi.org/10.1038/ngeo1922

Mühl, M., Schmitt, J., Seth, B., Lee, J.E., Edwards, J.S., Brook, E.J., Blunier, T., Fischer, H., 2023. Methane, ethane, and propane production in Greenland ice core samples and a first isotopic characterization of excess methane. Climate of the Past 19, 999–1025. https://doi.org/10.5194/cp-19-999-2023

Murray, L.T., Mickley, L.J., Kaplan, J.O., Sofen, E.D., Pfeiffer, M., Alexander, B., 2014. Factors controlling variability in the oxidative capacity of the troposphere since the Last Glacial Maximum. Atmos. Chem. Phys 14, 3589–3622.

Nisbet, E.G., Manning, M.R., Dlugokencky, E.J., Michel, S.E., Lan, X., Röckmann, T., Denier Van Der Gon, H.A.C., Schmitt, J., Palmer, P.I., Dyonisius, M.N., Oh, Y., Fisher, R.E., Lowry, D., France, J.L., White, J.W.C., Brailsford, G., Bromley, T., 2023. Atmospheric Methane: Comparison Between Methane's

Record in 2006–2022 and During Glacial Terminations. Global Biogeochemical Cycles 37, e2023GB007875. https://doi.org/10.1029/2023GB007875

Pedro, J.B., Jochum, M., Buizert, C., He, F., Barker, S., Rasmussen, S.O., 2018. Beyond the bipolar seesaw: Toward a process understanding of interhemispheric coupling. Quaternary Science Reviews 192, 27–46. https://doi.org/10.1016/j.quascirev.2018.05.005

Petit, J.-R., Jouzel, J., Raynaud, D., Barkov, N.I., Barnola, J.-M., Basile, I., Bender, M., Chappellaz, J., Davis, M., Delaygue, G., 1999. Climate and atmospheric history of the past 420,000 years from the Vostok ice core, Antarctica. Nature 399, 429–436.

Petrenko, V.V., Severinghaus, J.P., Brook, E.J., Mühle, J., Headly, M., Harth, C.M., Schaefer, H., Reeh, N., Weiss, R.F., Lowe, D., Smith, A.M., 2008. A novel method for obtaining very large ancient air samples from ablating glacial ice for analyses of methane radiocarbon. Journal of Glaciology 54, 233–244. https://doi.org/10.3189/002214308784886135

Rhodes, R.H., Brook, E.J., Chiang, J.C., Blunier, T., Maselli, O.J., McConnell, J.R., Romanini, D., Severinghaus, J.P., 2015. Enhanced tropical methane production in response to iceberg discharge in the North Atlantic. Science 348, 1016–1019. https://doi.org/10.1126/science.1262005

Rhodes, R.H., Brook, E.J., McConnell, J.R., Blunier, T., Sime, L.C., Fain, X., Mulvaney, R., 2017. Atmospheric methane variability: Centennial scale signals in the Last Glacial Period. Global Biogeochem. Cycles 2016GB005570. https://doi.org/10.1002/2016GB005570

Rhodes, R.H., Faïn, X., Brook, E.J., McConnell, J.R., Maselli, O.J., Sigl, M., Edwards, J., Buizert, C., Blunier, T., Chappellaz, J., Freitag, J., 2016. Local artifacts in ice core methane records caused by layered bubble trapping and in situ production: a multi-site investigation. Clim. Past 12, 1061–1077. https://doi.org/10.5194/cp-12-1061-2016

Rhodes, R.H., Faïn, X., Stowasser, C., Blunier, T., Chappellaz, J., McConnell, J.R., Romanini, D., Mitchell, L.E., Brook, E.J., 2013. Continuous methane measurements from a late Holocene Greenland ice core: Atmospheric and in-situ signals. Earth and Planetary Science Letters 368, 9–19. https://doi.org/10.1016/j.epsl.2013.02.034

Riddell-Young, B., Rosen, J., Brook, E., Buizert, C., Martin, K., Lee, J., Edwards, J., Mühl, M., Schmitt, J., Fischer, H., 2023. Atmospheric methane variability through the Last Glacial Maximum and deglaciation mainly controlled by tropical sources. Nature Geoscience 1–7.

Ringeval, B., Hopcroft, P.O., Valdes, P.J., Ciais, P., Ramstein, G., Dolman, A.J., Kageyama, M., 2013. Response of methane emissions from wetlands to the Last Glacial Maximum and an idealized Dansgaard–Oeschger climate event: insights from two models of different complexity. Climate of the Past 9, 149–171. https://doi.org/10.5194/cp-9-149-2013

Rosen, J.L., Brook, E.J., Severinghaus, J.P., Blunier, T., Mitchell, L.E., Lee, J.E., Edwards, J.S., Gkinis, V., 2014. An ice core record of near-synchronous global climate changes at the Bølling transition. Nature Geosci 7, 459–463. https://doi.org/10.1038/ngeo2147

Rubino, M., Etheridge, D.M., Thornton, D.P., Howden, R., Allison, C.E., Francey, R.J., Langenfelds, R.L., Steele, L.P., Trudinger, C.M., Spencer, D.A., Curran, M.A.J., van Ommen, T.D., Smith, A.M., 2019. Revised records of atmospheric trace gases CO_2, CH_4, N_2O, and $\delta^{13}C$-CO_2 over the last 2000 years from Law Dome, Antarctica. Earth System Science Data 11, 473–492. https://doi.org/10.5194/essd-11-473-2019

Ruddiman, W.F., 2003. The Anthropogenic Greenhouse Era Began Thousands of Years Ago. Climatic Change 61, 261–293. https://doi.org/10.1023/B:CLIM.0000004577.17928.fa

Sapart, C.J., Monteil, G., Prokopiou, M., van de Wal, R.S., Kaplan, J.O., Sperlich, P., Krumhardt, K.M., van der Veen, C., Houweling, S., Krol, M.C., Blunier, T., Sowers, T., Martinerie, P., Witrant, E., Dahl-Jensen, D., Rockmann, T., 2012. Natural and anthropogenic variations in methane sources during the past two millennia. Nature 490, 85–8. https://doi.org/10.1038/nature11461

Saunois, M., Stavert, A.R., Poulter, B., Bousquet, P., Canadell, J.G., Jackson, R.B., Raymond, P.A., Dlugokencky, E.J., Houweling, S., Patra, P.K., Ciais, P., Arora, V.K., Bastviken, D., Bergamaschi, P., Blake, D.R., Brailsford, G., Bruhwiler, L., Carlson, K.M., Carrol, M., Castaldi, S., Chandra, N., Crevoisier, C., Crill, P.M., Covey, K., Curry, C.L., Etiope, G., Frankenberg, C., Gedney, N., Hegglin, M.I., Höglund-Isaksson, L., Hugelius, G., Ishizawa, M., Ito, A., Janssens-Maenhout, G., Jensen, K.M., Joos, F., Kleinen, T., Krummel, P.B., Langenfelds, R.L., Laruelle, G.G., Liu, L., Machida, T., Maksyutov, S., McDonald, K.C., McNorton, J., Miller, P.A., Melton, J.R., Morino, I., Müller, J., Murguia-Flores, F., Naik, V., Niwa, Y., Noce, S., O'Doherty, S., Parker, R.J., Peng, C., Peng, S., Peters, G.P., Prigent, C., Prinn, R., Ramonet, M., Regnier, P., Riley, W.J., Rosentreter, J.A., Segers, A., Simpson, I.J., Shi, H., Smith, S.J., Steele, L.P., Thornton, B.F., Tian, H., Tohjima, Y., Tubiello,

F.N., Tsuruta, A., Viovy, N., Voulgarakis, A., Weber, T.S., van Weele, M., van der Werf, G.R., Weiss, R.F., Worthy, D., Wunch, D., Yin, Y., Yoshida, Y., Zhang, W., Zhang, Z., Zhao, Y., Zheng, B., Zhu, Qing, Zhu, Qiuan, Zhuang, Q., 2020. The Global Methane Budget 2000–2017. Earth System Science Data 12, 1561–1623. https://doi.org/10.5194/essd-12-1561-2020

Schilt, A., Baumgartner, M., Blunier, T., Schwander, J., Spahni, R., Fischer, H., Stocker, T.F., 2010a. Glacial-interglacial and millennial-scale variations in the atmospheric nitrous oxide concentration during the last 800,000 years. Quaternary Science Reviews 29, 182–192. https://doi.org/10.1016/j.quascirev.2009.03.011

Schilt, A., Baumgartner, M., Schwander, J., Buiron, D., Capron, E., Chappellaz, J., Loulergue, L., Schupbach, S., Spahni, R., Fischer, H., Stocker, T.F., 2010b. Atmospheric nitrous oxide during the last 140,000 years. Earth and Planetary Science Letters 300, 33–43. https://doi.org/10.1016/j.epsl.2010.09.027

Schmitt, J., Seth, B., Bock, M., Fischer, H., 2014. Online technique for isotope and mixing ratios of CH_4, N_2O, Xe and mixing ratios of organic trace gases on a single ice core sample. Atmospheric Measurement Techniques 7, 2645–2665. https://doi.org/10.5194/amt-7-2645-2014

Severinghaus, J.P., 1999. Abrupt Climate Change at the End of the Last Glacial Period Inferred from Trapped Air in Polar Ice. Science 286, 930–934. https://doi.org/10.1126/science.286.5441.930

Sherwood, O.A., Schwietzke, S., Arling, V.A., Etiope, G., 2017. Global Inventory of Gas Geochemistry Data from Fossil Fuel, Microbial and Burning Sources, version 2017. Earth Syst. Sci. Data 9, 639–656. https://doi.org/10.5194/essd-9-639-2017

Singarayer, J.S., Valdes, P.J., Friedlingstein, P., Nelson, S., Beerling, D.J., 2011. Late Holocene methane rise caused by orbitally controlled increase in tropical sources. Nature 470, 82–85.

Sowers, T., 2010. Atmospheric methane isotope records covering the Holocene period. Quaternary Science Reviews 29, 213–221. https://doi.org/10.1016/j.quascirev.2009.05.023

Sowers, T., Bernard, S., Aballain, O., Chappellaz, J., Barnola, J.-M., Marik, T., 2005. Records of the δ13C of atmospheric CH4 over the last 2 centuries as recorded in Antarctic snow and ice. Global Biogeochemical Cycles 19. https://doi.org/10.1029/2004GB002408

Spahni, R., Schwander, J., Fluckiger, J., Stauffer, B., Chappellaz, J., Raynaud, D., 2003. The attenuation of fast atmospheric CH4 variations recorded in polar ice cores. Geophysical Research Letters 30, 1571. https://doi.org/10.1029/2003gl017093

Stevenson, D.S., Zhao, A., Naik, V., O'Connor, F.M., Tilmes, S., Zeng, G., Murray, L.T., Collins, W.J., Griffiths, P.T., Shim, S., Horowitz, L.W., Sentman, L.T., Emmons, L., 2020. Trends in global tropospheric hydroxyl radical and methane lifetime since 1850 from AerChemMIP. Atmospheric Chemistry and Physics 20, 12905–12920. https://doi.org/10.5194/acp-20-12905-2020

Stowasser, C., Buizert, C., Gkinis, V., Chappellaz, J., Schüpbach, S., Bigler, M., Faïn, X., Sperlich, P., Baumgartner, M., Schilt, A., Blunier, T., 2012. Continuous measurements of methane mixing ratios from ice cores. Atmospheric Measurement Techniques 5, 999–1013. https://doi.org/10.5194/amt-5-999-2012

Svensson, A., Andersen, K.K., Bigler, M., Clausen, H.B., Dahl-Jensen, D., Davies, S.M., Johnsen, S.J., Muscheler, R., Parrenin, F., Rasmussen, S.O., Röthlisberger, R., Seierstad, I., Steffensen, J.P., Vinther, B.M., 2008. A 60 000 year Greenland stratigraphic ice core chronology. Clim. Past 4, 47–57. https://doi.org/10.5194/cp-4-47-2008

WAIS Divide Project Members, 2015. Precise interpolar phasing of abrupt climate change during the last ice age. Nature 520, 661–665. https://doi.org/10.1038/nature14401

Yin, Q., 2013. Insolation-induced mid-Brunhes transition in Southern Ocean ventilation and deep-ocean temperature. Nature 494, 222–225. https://doi.org/10.1038/nature11790

Websites

https://www.globalcarbonproject.org/methanebudget/
https://gml.noaa.gov/aggi/aggi.html